

行政院國家科學委員會補助專題研究計畫成果報告

共價鍵材料場發射顯示技術之研究—子計畫三：高功效鑽石場效發射顯示器(FED)元件之製作與特性分析

(III)

計畫類別：個別型計畫 整合型計畫

計畫編號：NSC 89-2216-E-009-042

執行期間：89年8月1日至90年7月31日

計畫主持人：陳家富

執行單位：國立交通大學材料科學與工程學系

中華民國 91 年 5 月 7 日

implies that samples grown under a bias less negative than -80V cause little carbon materials on the Pt films. Increasing the bias to -120V , it generates the high-density carbon nanotips.

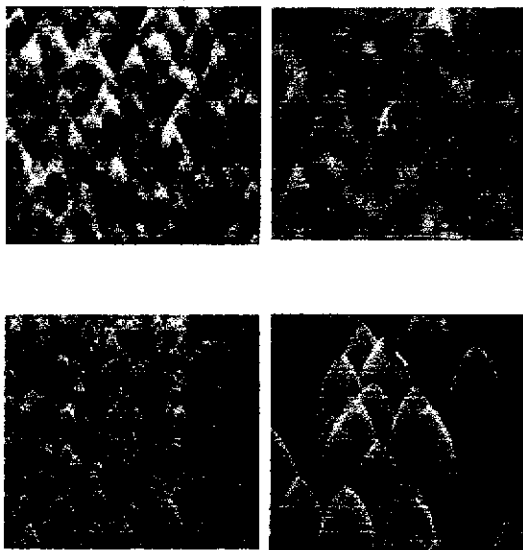


Figure 1

Fig. 2 shows these well-aligned carbon nanotips grown upward to $5.4\ \mu\text{m}$ length and $64\ \text{nm}$ in diameter under -120V . Sharper nanotips have a higher-aspect-ratio, indicating good characteristics for field emission. Fig. 1(b, however indicates that tips will grow to a sub-micrometer diameter under a higher bias (more negative than -120V), revealing that bias can enhance the growth of carbon nanotips on Pt films. Hence, the optimal bias for growing carbon nanotips on Pt films is -120V .



Figure 2

Figure 3 also shows good results of carbon nanotips grown on Si under -120V , but the deposition time is shorter than those grown on Pt films. This is due to the fact that it is easier to form carbon materials on Si than on Pt [9].



Figure 3

Figure 4 (a) displays the TEM images of an end section of an individual nanotip grown under -120V . Unlike hollow carbon nanotubes, carbon nanotips are solid. The main feature of note is the tip's somewhat irregular shape, with one primary protrusion. The diffraction pattern (DP) indicates that the end section is graphite. Moreover, Fig. 4 (b) displays the lateral section of the same tip, showing well-organized microcrystalline graphite section. The DP of Fig. 4 (b) also confirms the existence of well-organized microcrystalline graphite, proving that the carbon nanotips are made of graphite.

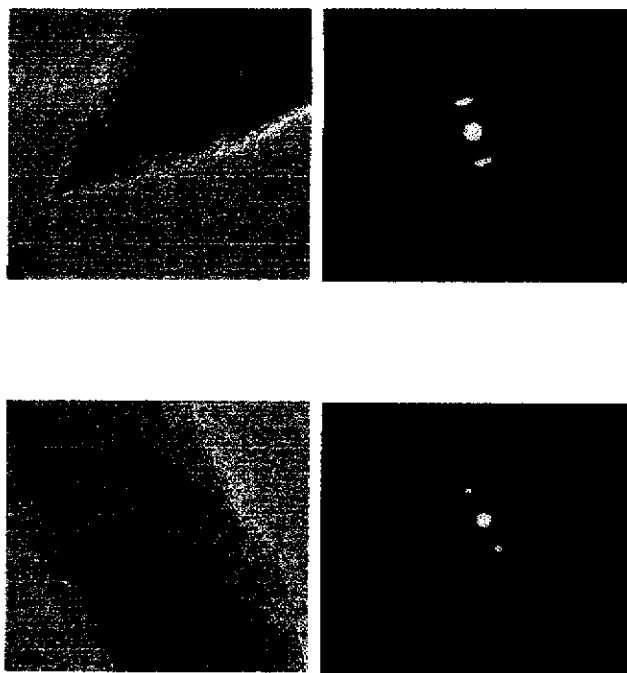


Figure 4

Figure 5 exhibits the Raman spectra of carbon nanotips grown under various bias and substrates. All of them have two sharp peaks located on about $1345\ \text{cm}^{-1}$ and $1580\ \text{cm}^{-1}$, respectively. The first-order Raman spectrum of aligned carbon nanotips shows

strong sharp peaks at 1581 cm^{-1} (G line), which is the high-frequency E_{2g} first-order mode and 1350 cm^{-1} (roughly corresponding to the D-line associated with disorder-allowed zone-edge modes of graphite). The peaks imply that the nanotips are characteristic of microcrystalline graphite. The relative intensities of the two peaks depend on the type of graphitic material. Normally, the intensity of the 1350 cm^{-1} peak increases (i) with an increase in the amount of unorganized carbon in the samples and (ii) with a decrease in the graphite crystal size [10].

The most conspicuous feature of carbon nanotips (grown under -120V) is that their Raman spectra show an additional weak peak at about 1618 cm^{-1} (D' line). The origin of the D and D' lines in other forms of carbon materials has been explained as disorder-induced features, caused by the finite particle size effect or lattice distortion [11-13]. Besides, a sample grown under -120V with a narrow bandwidth of the G-line and the D-line has well-organized carbon. The previous TEM image clearly displays the existence of well-organized graphite in the sample.

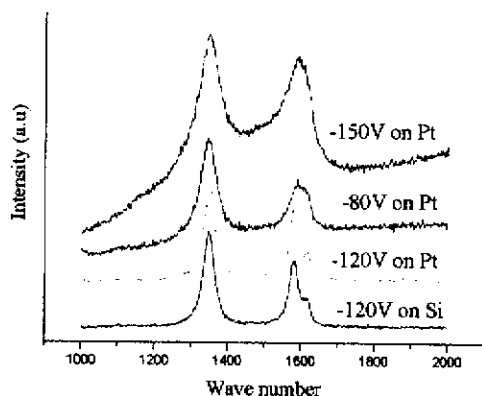


Figure 5

The field emission tests are performed on a diode structure, in which the carbon nanotips are separated from the anode, indium-tin-oxide glass, using $500\text{ }\mu\text{m}$ glass as spacers. The voltage-current (I - V) properties are measured and analyzed through the Fowler-Nordheim (FN) model, viz the $\ln(I/V^2)$ VS. $1/V$ plot. Fig. 6

characterizes carbon nanotips grown under -120V on Si and Pt. The current densities at $2.2\text{V}/\mu\text{m}$ of nanotips under -120V grown on Si and Pt are 761 and $617\text{ }\mu\text{A}/\text{cm}^2$, respectively. The threshold voltage (V_T) is defined as the intersection of the slope of F-N plots with abscissa. According to the F-N analysis, the emission behavior of the sample grown on the Pt films is better than that grown on Si. (lower turn-on field = $1.5\text{ V}/\mu\text{m}$). It is attributed to the presence of Pt layers, which provide a good conduction path for electrons to transport from the cathode to the emission sites [14].

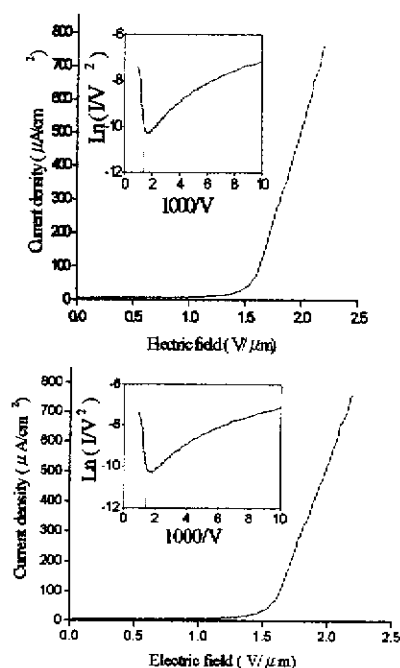


Figure 6

Reference

1. S.Iijima, Nature (London) **354**,56 (1991).
2. Z.L. Wang (Ed). , Characterization of Nanophase Materials. Wiley-VCH, New York, pp. 1-400(1999).
3. Chris Bower, Otto Zhou, Wei Zhu, D.J.Werder, and Sungho Jin. Appl. Phys. Lett, **77**, 2767(2000).
4. J.Kim, K.No, and C.J.Lee, J. Appl. Phys, **90**,2591(2001).
5. J.I.Sohn, S.Lee, .H.Song, .Y.Choi,K.L.Cho, and K.S.Nam, Appl.Phys.Lett, **78**, 901(2001).
6. S.Yugo, T.Kanai, T.Kimura and T.Muto,

- Appl. Phys. Lett, **58**, 1036 (1991).
7. Huang, J.T.; Yeh, W.Y.; Hwang, J.; Chang, H. Thin Solid Films **315**, 35 (1998).
 8. Stöckel, R.; Janischowsky, K.; Rohmfeld, S.; Ristein, J.; Hundhausen, M.; Ley, L. Diam.Relat.Mat **5**, 321 (1996).
 9. T. Tachibana, Y. Yokota, K. Hayashi, K. Miyata, K. Kobashi and Y. Shintani Diam. Relat. Mater., **9**, 251 (2000).
 10. F. Tuinstra and J.L.Koenig, J.Chem.Phys. **53**, 1126(1970).
 11. G. Vitali, M. Rossi, M. L. Terranova, and V. Sessa, J. Appl. Phys. **77**, 4307 (1995).
 12. D. G. McCulloch, S. Praver, and A. Hoffman, Phys. Rev. B **50**, 5905 (1994).
 13. V. Barbarossa, F. Galluzzi, R. Tomaciello, and A. Zanobi, Chem. Phys. Lett. **185**, 53 (1991).
 14. J.S.Lee;K.S.LiuandI.N.Lin, Appl.Phys.Lett. **71**, 554 (1997).